The thermal behaviour of three different auger pressure grouted piles used as heat exchangers

*Fleur Loveridge, University of Southampton, Highfield, Southampton, SO17 1BJ, U.K., Fleur.Loveridge@soton.ac.uk, 0044(0)2380595459

C. Guney Olgun, Virginia Tech, Blacksburg, VA, 24061, U.S.A., colgun@vt.edu, 001-540-231-2036

Tracy Brettmann, A. H. Beck Foundation Co., Inc, Houston, USA, tracy.brettmann@ahbeck.com, 001 713 413 3800

William Powrie, University of Southampton, Highfield, Southampton, SO17 1BJ, U.K., wp@soton.ac.uk, 0044(0)2380593214

* corresponding author

Symbols and Abbreviations Used

APG	auger pressure grouted pile
APGE	auger pressure grouted energy pile
AR	aspect ratio
Fo	Fourier number (non-dimensional time)
G	G-function
G_c	Concrete G-function
G_g	Pile G-function
H	pile length
h_i	heat transfer coefficient
$\dot{m}$	mass flow rate
n	number of pipes
q	applied power per metre depth
R_b	pile or borehole resistance
R_c	concrete resistance
R_p	pipe resistance
R_{pcond}	pipe conductive resistance
R_{pconv}	pipe convective resistance
RMSE	root mean square error
r_b	pile or borehole radius
r_i	pipe inner radius
r_o	pipe outer radius
S_c	specific heat capacity OR shape factor
s	shank spacing
T	temperature
ΔT	change in temperature
T_{in}	pile entering temperature
T_{out}	pile leaving temperature
t	time
TG	thermal grout
α_g	thermal diffusivity of ground
Φ_f	dimensionless fluid temperature change
Φ_g	dimensionless temperature change in the ground.
γ	Euler's Constant
λ_c	thermal conductivity of concrete/grout
λ_g	thermal conductivity of ground
λ_p	thermal conductivity of pipe material

The thermal behaviour of three different auger pressure grouted piles used as heat exchangers

Abstract

Three auger pressure grouted (APG) test piles were constructed at a site in Richmond, Texas. The piles were each equipped with two U-loops of heat transfer pipes so that they could function as pile heat exchangers. The piles were of two different diameters and used two different grouts, a standard APG grout and a thermally enhanced grout. Thermal response tests, where fluid heated at a constant rate is circulated through the pipe loops, were carried out on the three piles, utilising either single or double loops. The resulting test data can be used to determine the surrounding soil thermal conductivity and the pile thermal resistance, both essential design parameters for ground source heat pump schemes using pile heat exchangers. This paper uses parameter estimation techniques to fit empirical temperature response curves to the thermal response test data and compares the results with standard line source interpretation techniques. As expected, the thermal response tests with double loops result in smaller thermal resistances than the same pile when the test was run with a single loop. Back analysis of the pile thermal resistance also allows calculation of the grout thermal properties. The thermally enhanced grout is shown to have inferior thermal properties than the standard APG grout. Together these analyses demonstrate the importance of pile size, grout thermal properties and pipe positions in controlling the thermal behaviour of heat exchanger piles. (229 words)

Keywords

Ground source heat pumps; piling; pile heat exchangers; thermal properties; thermal response tests.

1 Introduction

The use of piled foundations as heat exchangers in a ground source heat pump system was first implemented in Austria in the 1980's (Brandl, 2006). Since then the use of "energy piles" has spread all over the world (e.g. Koene et al, 2000, Pahud & Hubbuch, 2007, Gao et al., 2008). While this technology is now being employed more routinely and is starting to be represented in codes and standards (e.g NHBC, 2010, GSHPA, 2012) there is still scope for improving design and analysis methods (e.g. Bourne-Webb et al., 2013, Loveridge & Powrie, 2013). In particular most thermal design proceeds on the basis of two key input parameters: the pile thermal resistance (R_b) and the surrounding soil thermal conductivity (λ_g). The soil thermal conductivity is an important parameter for controlling the transient temperature changes in the ground, while the pile thermal resistance governs the temperature change between the heat transfer fluid circulating within pipes installed in the pile and pile edge. λ_g and R_b are often determined in situ using a thermal response test, where a controlled amount of heating power is applied to the pile heat exchanger and the temperature response of the circulating fluid is monitored.

This paper will focus on the thermal response testing of three auger pressure grouted energy (APGE) piles constructed by Berkel & Company at a site near Richmond in Texas. Two different models to describe the temperature change within and around the pile will be used to back analyse the tests and determine the ground thermal conductivity and pile thermal resistance. Variations in the calculated values and differences between the observed and modelled behaviour are then used to examine how the size of the pile, its material properties and the arrangement of heat transfer pipes within the pile cross section may affect the pile thermal behaviour.

2 Pile Heat Exchanger Models

Before examining the pile thermal response tests in detail it is necessary to review the main models used in the analysis and design of pile heat exchangers. These are used primarily to predict the temperature change of the circulating fluid for given thermal loads and properties. However, the models can also be applied to the inverse problem of interpreting thermal response tests data.

Based on the practice that has become established for more common borehole heat exchangers, it is usual to split the temperature change which occurs within the pile (the internal response) from that within the surrounding ground (the external response) and then to sum the results of the two separate calculations to obtain the total temperature change of the fluid. Alternatively it is possible to solve both parts of the problem together using more advanced analytical or numerical models (e.g. Javed & Claesson, 2011, Li & Lai, 2012, Park et al., 2013, Zarrella et al., 2013). The section below first addresses the external and internal responses separately and then the potential for a combined analysis.

2.1 External Response

The most commonly used techniques to predict the temperature change in the ground around a vertical (e.g pile or borehole) ground heat exchanger are the line, hollow cylinder and solid cylinder source models. These models solve the heat diffusion equations for a heat source of a given geometry, either assuming that the heat source is effectively infinite (to allow the use of 2D cylindrical coordinates) or assuming that the heat source is finite (a full 3D solution). All models assume that the ground is of uniform initial temperature, and in the case of the 3D solutions, that the ground surface is fixed at this temperature. Full solutions for these models are given in Carslaw & Jaeger, 1959 (infinite line source); Eskilson, 1987, Diao et al., 2004 (finite line source); Ingersoll et al., 1954, Bernier, 2001 (hollow cylinder models); and Man et al. 2010 (solid cylinder models), with a graphical representation of the "infinite" models given in Figure 1. The curves shown in Figure 1 are often known as temperature response functions and are plotted as non-dimensional ground temperature change ($\Phi_g = 2\pi\lambda_g \Delta T_g / q$) against non-dimensional time ($Fo = \alpha_g t / r_b^2$) for a constant applied thermal load. In this notation ΔT is the change in temperature, α is the thermal diffusivity (m^2/s), t is the elapsed time (s), r_b is the heat exchanger radius (m) and q is the applied thermal load per unit depth of the heat exchanger (W/m). The subscript g represents the ground.

Figure 1 The main models for ground heat exchanger external thermal response

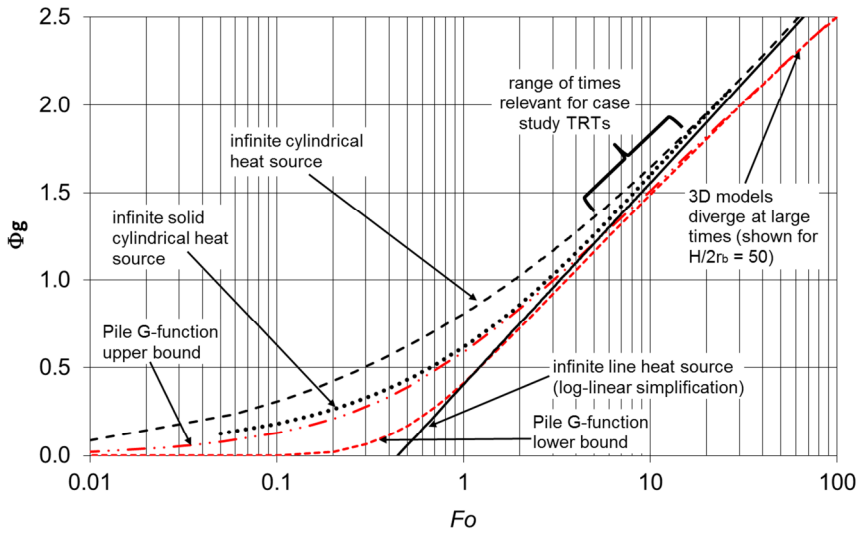

The non-dimensional approach allows comparison of the performance of piles of different sizes with different applied thermal loads, as will be seen later in Figure 5. Also plotted on Figure 1 is a pair of empirical temperature response functions known as pile G-functions (Loveridge & Powrie, 2013). These give upper and lower bound solutions based on a range of numerical simulations designed to cover a realistic range of common

pile heat exchanger geometries. It can be seen that these functions lie between the line source model and the solid cylinder model at short times (Fo<1). As the G-functions are based on a finite pile geometry they then predict temperature changes less that the infinite heat exchanger models at larger values of time as the influence of the surface boundary condition becomes apparent. The degree of divergence from the infinite heat source models depends on the elapsed time and the aspect ratio (AR) of the heat exchanger, where AR=H/2r_b with H being the length of the heat exchanger and r_b the radius. The case shown in Figure 1 is for AR=50. At larger values of time than shown in Figure 1, all of the "finite" heat source models (i.e. the finite line, finite cylinder and G-functions) converge to the same steady state value of Φ_g, with that value determined by the pile aspect ratio.

2.2 Internal Response

The majority of ground heat exchanger analyses assume that there is a thermal steady state within the heat exchanger. This means that the difference between the average temperature of the fluid circulating in the heat transfer pipes and the average temperature of ground at the edge of the heat exchanger is constant, and can therefore be characterised by a constant steady state resistance. This is a reasonable assumption for small diameter heat exchangers such as boreholes where the thermal mass of the grout is small. However, in pile heat exchangers, depending on their size, this assumption is usually invalid and the concrete or grout may take a numbers of days to reach steady state (Loveridge & Powrie, 2014). As a result, new concrete G-functions have been proposed to allow calculation of the temperature changes within the pile as a function of time (Loveridge & Powrie, 2013). These functions depend on the pile geometry and examples are given in Figure 2, which shows how the resistance of the concrete part of the pile (R_c) increases with Fo.

Figure 2 Range of concrete G-functions, assuming pipes placed centrally within a pile (after Loveridge & Powrie, 2013)

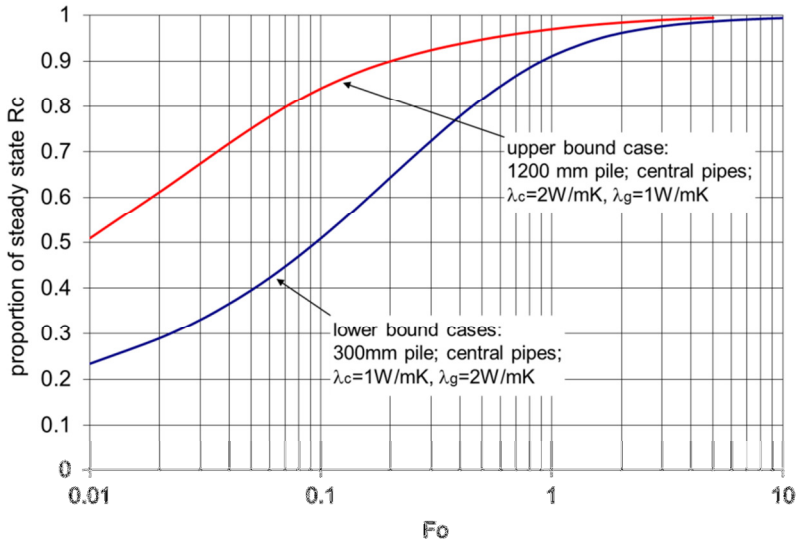

Both approaches still require calculation of the pile thermal resistance, R_b, but the concrete G-function allows part of this (R_c) to be a transient rather than a steady state value (Figure 2). Steady state pile thermal resistance is usually determined as the sum of its component resistances as follows:

$$R_b = R_c + R_{pcond} + R_{pconv} \qquad \textbf{Equation 1}$$

R_{pconv} is the resistance associated with convection within the pipe circuit. This can be calculated (Equation 2) based on the number of pipes (n), their internal radius (r_i) and the heat transfer coefficient h_i determined, for example, using the Gnielinksi correlation (Gnielinski, 1976) assuming turbulent flow:

$$R_{pconv} = \frac{1}{2n\pi r_i h_i} \qquad \textbf{Equation 2}$$

R_{pcond} is the resistance associated with conduction through the pipe material. It can be calculated by assuming a value for the thermal conductivity of the pipe material (λ_p), and using the equation for the thermal resistance of a cylinder of external radius r_o:

$$R_{pcond} = \frac{ln(r_o/r_i)}{2n\pi\lambda_p} \qquad \textbf{Equation 3}$$

R_c is the resistance associated with the concrete or grout part of the pile. Its steady state value can also be calculated using the equation for the thermal resistance of a cylinder (same form as Equation 3), but an assumption must be made regarding the effective inner radius of that cylinder r_{eff}, (to replace r_i in Equation 3). Shonder & Beck (2000) suggest that this value can be taken as $r_{eff} = r_o\sqrt{n}$. Alternatively, the more accurate multipole method for determining R_c may be used (Bennet et al., 1987). This is based on superposition of individual poles (complex number equivalents of line sources) which represent the position of each pipe in the heat exchanger. When many pipes are present, the solution is mathematically complicated. However, for the two pipe case the equations are simple, especially if a line source rather than a multipole assumption is made; full details are given in Hellstrom (1991). A set of empirical equations for calculating R_c proposed by Loveridge & Powrie (2014), based on numerical models of pile heat exchangers, can also be used for a range of pipe configurations. Once the steady state value of R_c has been determined, Figure 2 can be used to model the transient behaviour.

2.3 Combined Models

A few models allow the temperature changes within the ground and the pile to be calculated together. For example, Li & Lai (2012) have developed analytical models that superimpose line sources in composite media for each heat transfer pipe in a pile heat exchanger. Their solutions are potentially mathematically very accurate but the exact solution must be derived for each specific geometry used. Javed & Claesson (2011) developed a 2D analytical model for borehole heat exchangers that solves the diffusion equation for the grout and ground together. However, it neglects three dimensional effects and simplifies the heat exchanger to an equivalent cylinder; it is not yet known how well this approach will extend to piles. Alternatively numerical models are available such as that developed and implemented by Zarrella et al. (2013) specifically for use with pile heat exchanger applications.

3 Berkel Test Site

Berkel & Company have developed an APGE test site at their regional offices in Richmond, Texas (Brettmann et al., 2010; Brettmann and Amis, 2011). Three piles were constructed using auger pressure grouted (or continuous flight auger) techniques to a depth of 18.3m (60 foot). Each pile was equipped with two 25mm (or 1 inch) polyethylene U-loops. The pipes were attached to the outside of a series of 127mm (or 5 inch) diameter spacers installed on a 25mm (or 1 inch) diameter steel bar (Figure 3). Two piles were augered at 305mm (or 12 inch) diameter and one pile at 457mm (or 18 inch) diameter. One of the 305mm piles was backfilled with low density thermal grout (TG), as typically used for borehole heat exchanger applications, and the other two piles were constructed using standard APGE cementitious grout. The piles were arranged in a triangular pattern with a borehole drilled in the centre for soil sampling (Figure 4).

Ground conditions at the site are a sequence of silts, sands and clays as shown in Figure 4. The groundwater table is estimated to be approximately 3.3m below ground level, although no significant groundwater flow is present at the site. Samples taken from the borehole were used to determine the moisture content and the soil thermal conductivity using a needle probe (ASTM, 2005); the results are given in Table 1. The weighted average thermal conductivity from the laboratory tests over the pile depth is 2.98 W/mK. Also included in Table 1 are the results of needle probe tests on samples of the two grouts used in pile construction.

Figure 3 Arrangement of heat transfer pipes within the test piles. Shown to scale for 305mm pile (left) and 457mm pile (right)

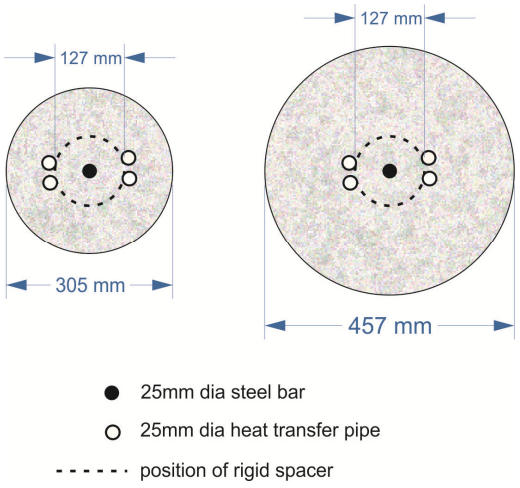

Figure 4 Pile layout and ground conditions (after Loveridge et al., 2014a)

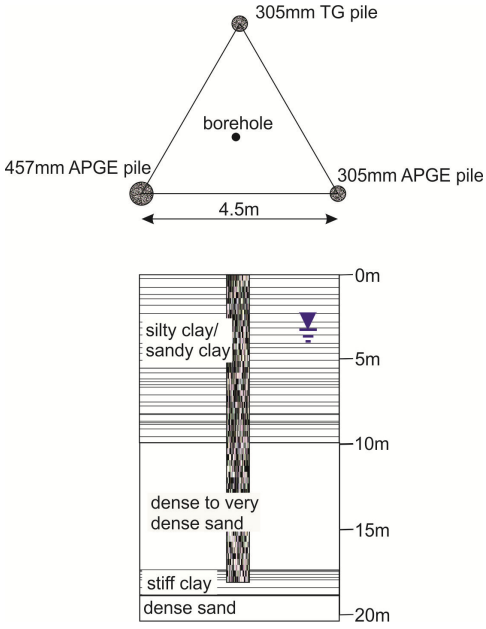

Table 1 Soil and grout laboratory test results (after Brettmann et al., 2010)

Sample (depth)	Moisture content	Density	Thermal conductivity
Clay (6.1m)	21.1 %	1.73 Mg/m^3	2.22 W/mK
Sand (13.7m)	14.0 %	1.73 Mg/m^3	4.05 W/mK
Clay (18.3m)	28.0 %	1.54 Mg/m^3	2.09 W/mK
APGE Grout	7.3 %	1.91 Mg/m^3	1.35 W/mK
Thermal Grout	64.5 %	0.93 Mg/m^3	1.35 W/mK

3.1 Thermal Response Tests

Five thermal response tests were carried out at the site (Brettmann et al., 2010); one on each of the three piles using both of the U-loops (referred to as a double test), and two tests on the APGE piles using only one of the U-loops (referred to as a single test). In each test power was supplied to the U-loop(s) within the pile at a nominally constant rate, while the temperature change of the fluid circulating within the pipes was recorded at the inlet and the outlet. The mean of these two temperatures was then used to represent the average fluid

temperature of the heat exchanger. Table 2 gives the characteristics of each test, including the power supplied to the pile calculated from:

$$\boldsymbol{Q = S_c \dot{m}(T_{in} - T_{out})} \qquad \textbf{Equation 4}$$

where Q is the total power supplied (in Watts), S_c is the specific heat capacity of the fluid (J/kgK), $\dot{m}$ is the mass flow rate (kg/s) and T_{out} and T_{in} are the outlet and inlet temperatures respectively. This shows that although nominally constant, there is actually significant variability in the power supplied. In addition, these variations fall outside of the range recommended by ASHRAE (2007), which requires the standard deviation of the power supplied to be less than 1.5% of the mean value. Furthermore, in the case of the 305mm APGE Single test and the 457mm APGE Double test particularly large power peaks/troughs occurred towards the end of the test (see also Figure 5). Due to the unreliability in recording of these spikes, analysis was only carried out on the test data prior to these times (Table 2).

Table 2 Test details and power supplied

Pile	Loops	Mean power	Power, standard deviation	Power, standard deviation as % of mean	Flow Rate	R_p	Test duration	Test duration analysed
305mm TG	Double	1484 W	103 W	6.9 %	1.24 m/s	0.0043 mK/W	94 hrs	94 hrs
305mm APGE	Double	2171 W	129 W	5.9 %	1.06 m/s	0.0044 mK/W	96 hrs	96 hrs
305mm APGE	Single	1609 W	133 W	8.3 %	1.31 m/s	0.0085 mK/W	96 hrs	67 hrs
457mm APGE	Double	2161 W	128 W	5.9 %	1.07 m/s	0.0044 mK/W	140 hrs	100 hrs
457mm APGE	Single	1616 W	134 W	8.3 %	1.34 m/s	0.0085 mK/W	110 hrs	110 hrs

Figure 5 Normalised temperature responses for the five thermal response tests

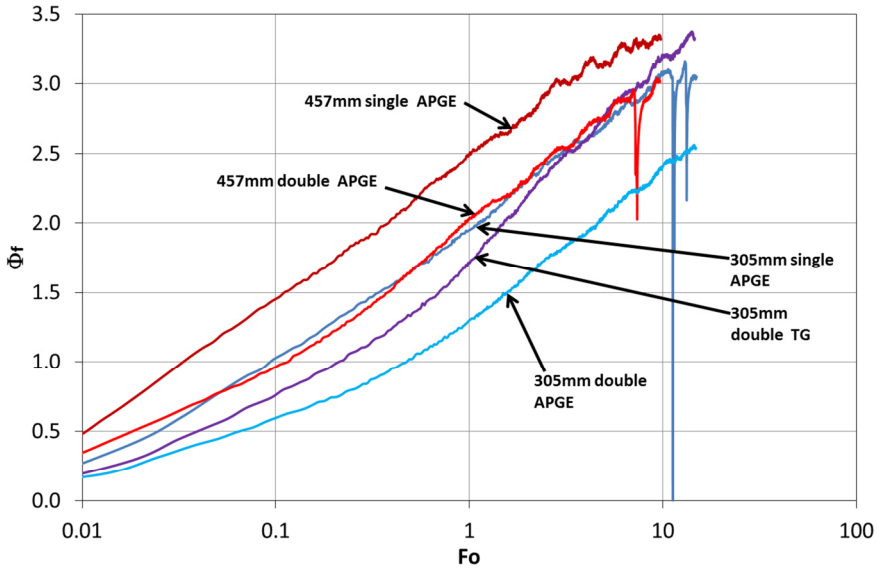

The average fluid temperature change ($\Phi_f = 2\pi\lambda_g \Delta T_f / q$) for the five tests is plotted non-dimensionally in Figure 5. Initially, when the temperature response is being controlled by the pile characteristics, the gradient and shape of the curves are all different, reflecting the different pipe configurations, pile sizes and pile grout materials. Later in the tests, however, the curves all have a similar gradient, reflecting the time when the temperature response is controlled by the ground thermal properties. The different normalised fluid temperature

change reached at the end of each test is a reflection of the different thermal resistances of the five configurations. Unsurprisingly the smaller piles have a lower resistance and plot on the lower half of the chart, while the larger pile has a higher resistance and plots in the upper half. Double loop tests also show smaller resistance (and hence temperature change) compared to single loop tests. Finally it can be seen that the thermal grout must have a lower thermal conductivity than the cementitious APGE grout as this pile has a higher resistance than its APGE counterpart of the same diameter.

4 Analysis Methods

4.1 Thermal Response Tests Interpretation

Two models have been chosen to analyse the data. First the infinite line source model which is most commonly applied in practice and secondly the pile and concrete G-functions which should theoretically better represent the pile behaviour. In both cases, the ground around the heat exchanger is assumed to be homogenous and isotropic with no moving groundwater. Therefore, the resulting value of λ_g obtained from the tests is sometimes referred to as an effective thermal conductivity as it is i) a lumped parameter for all geological units crossed by the heat exchanger and ii) includes the influence of groundwater flow, if there is any. While the latter is not relevant in this case, λ_g determined for pile heat exchangers can include the influence of the pile concrete or grout as will be discussed in Section 6.

4.1.1 Infinite Line Source Model

The equation for the infinite line source can be presented as a log-linear relationship (Equation 5), which easily allows determination of λ_g and R_b from a graph of temperature change against the logarithm of time.

$$\Delta T_f = qR_b + \frac{q}{4\pi\lambda_g}\left(\ln\left(4\alpha_g t / r_b^2\right) - \gamma\right) \qquad \textbf{Equation 5}$$

where ΔT_f is the average temperature change of the circulating fluid and γ is Euler's constant. The first term gives the pile internal response in terms of the resistance R_b, while the second term gives the external ground response. However, the second term in Equation 5 is the simplification of the full solution to the diffusion equations and is only valid at large values of time, defined as when $Fo > 5$ or when $t > 5r_b^2/\alpha_g$. Fulfilment of this criterion limits the difference between the simplified solution and the full solution to less than 10% (Hellstrom, 1991). Consequently when using the line source model to interpret thermal response test data it is usual to use only the portion of the test data that complies with this criterion. For borehole heat exchangers this may be after only a few hours, but for pile heat exchangers which have a larger diameter, this initial time period may extend to a day or more. For the 305mm piles $Fo = 5$ is equivalent to approximately 32 hours, while for the 457mm pile it corresponds to 73 hours, the latter in particular being a large proportion of the total test duration. In fact, given that many tests are conducted over 60 hours or less, this would restrict the use of the line source model for larger piles.

In this paper we will use both the full dataset and that restricted to Fo>5 to compare the two outcomes.

4.1.2 Pile and Concrete G-functions

To apply the pile and concrete G-functions the following equation is used:

$$\Delta T_f = qR_p + qR_cG_c + \frac{q}{2\pi\lambda_g}G_g \qquad \textbf{Equation 6}$$

where $R_p = R_{pcond} + R_{pconv}$, and the pile G-function G_g and the concrete G-function G_c, take the form:

$$G = a[\ln(Fo)]^7 + b[\ln(Fo)]^6 + c[\ln(Fo)]^5 + d[\ln(Fo)]^4 + e[\ln(Fo)]^3 + f[\ln(Fo)]^2 + g[\ln(Fo)]\ h$$

Equation 7

with a to h being constants, the values of which are given in Table 3. In this case the constants have been chosen for the case of a lower bound pile (one where the grout is expected to be less conductive than the ground) with an aspect ratio of approximately 50. This curve is plotted in Figure 1. The concrete G-function additionally assumes that the pipes are placed near the centre of the pile. Full details of the pile and concrete G-functions are given in Loveridge & Powrie (2013).

Table 3 Values of the empirical constants used with the pile and concrete G-functions (after Loveridge & Powrie, 2013)

Empirical Constant	Pile G-function (lower bound, AR=50)[1]	Concrete G-function (lower bound for pipes near the pile centre)[2]
a	-8.741×10^{-8}	0
b	8.243×10^{-6}	-1.01×10^{-4}
c	-1.835×10^{-4}	-2.34×10^{-4}
d	1.894×10^{-3}	3.037×10^{-3}
e	-0.01375	1.803×10^{-3}
f	0.04905	-0.04339
g	0.3997	0.1029
h	0.4267	0.9095

Notes: (1) For Fo<0.25, G=0; (2) For Fo<0.01, G=0; and for Fo>10, G=1.

4.1.3 Direct and Superposition Analysis

Earlier work on the Berkel & Company tests (Loveridge et al., 2014a) has shown how the variations in applied power (Table 2) can give rise to uncertainty in the results. The line source method was previously applied directly (assuming constant power), using different subsets of the test data to see how the results varied with time. In most cases this step-wise analysis approach did not produce consistent results owing to the influence of pile size and variable power input. Therefore in this paper, as well as directly applying the above models assuming that q is constant, superposition of the real power time series has been carried out by application of the following equation:

$$\Delta T_n = \sum_{i=1}^{i=n} \frac{q_i}{2\pi\lambda_g}\left[G\left(Fo_n - Fo_{(i-1)}\right) - G\left(Fo_n - Fo_i\right)\right] \qquad \textbf{Equation 8}$$

where n is the point in normalised time in which the superposition is evaluated and G is a function calculated at the value of Fo prescribed in the equation. For the pile and concrete G-functions G is given by Equation 7. For the line source model G is the function for the ground temperature change, following from the second term in Equation 5:

$$G = \frac{1}{2}(ln\{4Fo\} - \gamma) \qquad \textbf{Equation 9}$$

Superposition of heat exchanger models in this way has been shown to be a successful method of handling variable power input, and been able to reproduce the results of more time consuming numerical analysis to an acceptable level (Sauer, 2013).

Owing to the additional computation involved in Equation 8, a parameter estimation approach must be carried out and the sum has been coded in Matlab to streamline this process. As direct application of the models is much quicker– it can be done graphically for the line source model and using the MS Excel SOLVER function for the G-functions – this has also been carried out for comparison purposes.

4.2 Derivation of Grout Thermal Conductivity

The empirical and analytical approaches for determining R_b can also be used to back calculate the concrete or grout conductivity (λ_c) from the results of the in situ thermal response tests. For the single loop tests the line source method for two pipes (Hellstrom, 1991) has been used to calculate the grout conductivity:

$$R_c = \frac{1}{4\pi\lambda_c}\left[\ln\left(\frac{r_b}{r_o}\right)+\ln\left(\frac{r_b}{s}\right)+\sigma\ln\left(\frac{r_b^{\,4}}{r_b^{\,4}-\left(s/2\right)^4}\right)\right] \qquad \textbf{Equation 10}$$

where

$$\sigma = \frac{\lambda_c - \lambda_g}{\lambda_c + \lambda_g} \qquad \textbf{Equation 11}$$

and s is the shank spacing, the centre to centre distance between the two pipes. For the double loop tests the empirical approach of Loveride & Powrie (2014) has been applied:

$$R_c = \frac{1}{\lambda_c S_c} \qquad \textbf{Equation 12}$$

Where S_c is a shape factor given by:

$$S_{c(steady)} = \frac{A}{B\ln\left(\frac{r_b}{r_o}\right)+C\ln\left(\frac{r_b}{c}\right)+\left(\frac{r_b}{r_o}\right)^D+\left(\frac{r_b}{c}\right)^E+F} \qquad \textbf{Equation 13}$$

with A to F being empirical constants given in Table 4. The values of the constants are chosen to represent the case of a pile with 4 pipes installed, assuming that the ground is more conductive than the pile grout. Full details are given in Loveridge & Powrie (2014). In both cases $R_b = R_c + R_p$, with values for R_p (calculated according to Equations 1 to 3) given in Table 2.

Table 4 Values of empirical constants for determining R_c (after Loveridge & Powrie, 2014)

	A	B	C	D	E	F
Pile with 4 pipes, assuming $2\lambda_c=\lambda_g$	3.369	0.1091	-0.09659	-11.79	-3.032	0.1535

5 Results

Tables 5 and 6 present the values of effective thermal conductivity and pile thermal resistance derived from the analysis of the thermal response tests, with a quantification of the model fit errors included in Table 7. These values are also represented graphically in Figures 6, 7 and 8.

5.1 Thermal Conductivity

With the exception of the 305mm thermal grout pile and the direct application of the models to the 457mm APGE single loop test, the effective thermal conductivity results are fairly consistent, averaging 3.10 W/mK. Most values are within 10% of this figure. On the other hand, the test on the 305mm thermal grout pile gives much lower thermal conductivities, averaging 2.4 W/mK, while direct application of the models to the 457mm APGE shows some much higher values and little consistency.

A greater insight into the reliability of the calculated thermal conductivity values can be obtained by considering the fit of the models to the measured test data. Table 7 and Figure 8 present the model fit errors in terms of root mean square error (RMSE), while Figure 9 compares the model fits for the calculated thermal parameters (for direct model application) with the measured temperature changes. The line source model fitted to the entire dataset consistently shows the highest errors, with an average RMSE of 0.35, compared with 0.17 for the line

source with Fo>5 and 0.22 for the G-functions. Although the line source model for Fo>5 does have smaller errors than the G-functions when the shapes of the curves are examined (Figure 9) the G-functions clearly provide a better fit to the measured data at small values of time where the transient behaviour within the pile is being correctly accounted for.

Interestingly the tests performed on double loops (Figure 9a, b & d) show excellent fit to the G-functions at small values of time, with the model providing a close match to the early curvature of the data set. The single loop tests, however, give a much straighter response overall and hence a better fit to the line source model (Figure 9c & e). For the case of the 457mm pile, where discarding data for Fo<5 means ignoring three quarters of the test data, the line source is rather misleading (Figure 9d & e).

A similar pattern is seen in Figure 10, which plots the modelled and measured data for the approach using superposition of the thermal power. The advantage of superposition can particularly be seen for the 457mm pile where only a short period of data is available for Fo>5. This means that in the direct application of the model variation in the power supplied over this period can significantly affect the outcome. However, in analysis with superposition of the power, a much better result is obtained.

Despite the superposition approach taking into account all the changes in power supplied to the piles, it does not give smaller model errors than the direct application (Table 7). This is because the models either assume that there is a constant temperature difference between the fluid and the ground (line source model) or that there is a constant temperature difference between the fluid and the grout (G-functions). In such cases all variations in power are directly transferred to the ground or grout respectively. In reality there will be some damping of the shortest timescale variations in power that is not reflected in either model and is causing the additional errors in the model fitting.

5.2 Thermal Resistance

Average values of R_b determined from the thermal response test using the various analyses are given for each pile in Table 6. Typically the ranges of results are within 10% of the average, with some additional variability seen for the Thermal Grout pile and the 457mm single loop test. The relative magnitudes of the resistance values are generally in keeping with that expected from the positions of the non-dimensional temperature response curves in Figure 5. The exception to this is the TG pile which plotted at the same level as the 305mm APGE pile (single loop test) and the 457mm APGE (double loop test). While the latter two piles have the same average calculated thermal resistance (0.104 mK/W), the 305mm TG pile only has a calculated resistance of 0.083 mK/W. This suggests that there is a much larger error in the calculation of the resistance for this pile (and this is no surprise as it has already been observed that erroneous or misleading values of λ_g are also calculated).

One possible explanation for this discrepancy is that as well as being of lower thermal conductivity than the APGE grout, the thermal grout is also of much lower diffusivity. This could mean that the pile is being influenced much more by its transient behaviour. Currently the G-function models assume that the ground and grout are of similar volumetric heat capacity and any difference in diffusivity are driven by the difference in thermal conductivity. However, in this case we know that the density of the thermal grout is approximately half that of the cementitious APGE grout (Table 1), which will have a large impact on its thermal diffusivity.

Table 5 Effective thermal conductivity values derived from the thermal response tests

		Direct determination			Superposition			Average values
Pile	Loops	Line all	Line Fo>5	G-function	Line all	Line Fo>5	G-function	
305mm TG	Double	2.38	2.47	2.22	2.40	2.60	2.15	2.37
305mm APGE	Double	3.26	2.90	2.84	3.20	3.50	2.90	3.10
305mm APGE	Single	2.86	2.58	2.96	3.15	2.90	3.45	2.98
457mm APGE	Double	2.93	3.25	3.10	3.05	3.55	3.20	3.18
457mm APGE	Single	3.29	5.46	4.31	3.00	3.00	3.55	3.77
Average Values		2.94	3.33	3.09	2.96	3.11	3.05	3.08

Table 6 Pile thermal resistance values derived from the thermal response tests

		Direct determination			Superposition			Average values
Pile	Loops	Line all	Line Fo>5	G-function	Line all	Line Fo>5	G-function	
305mm TG	Double	0.0816	0.0877	0.0808	0.0818	0.0918	0.0768	0.083
305mm APGE	Double	0.0631	0.0551	0.0579	0.0619	0.0694	0.0594	0.061
305mm APGE	Single	0.1006	0.0925	0.1078	0.1060	0.1010	0.1160	0.104
457mm APGE	Double	0.0973	0.1034	0.1055	0.0994	0.1094	0.1069	0.104
457mm APGE	Single	0.1269	0.1569	0.1453	0.1210	0.1210	0.1360	0.135

Table 7 Root mean square error values for the model fitting

		Direct determination			Superposition			Average values
Pile	Loops	Line all	Line Fo>5	G-function	Line all	Line Fo>5	G-function	
305mm TG	Double	0.321	0.112	0.137	0.458	0.256	0.173	0.24
305mm" APGE	Double	0.594	0.122	0.153	0.453	0.231	0.141	0.28
305mm APGE	Single	0.176	0.120	0.175	0.326	0.276	0.418	0.25
457mm APGE	Double	0.302	0.154	0.173	0.358	0.126	0.263	0.23
457mm APGE	Single	0.276	0.139	0.211	0.283	0.176	0.379	0.24
Average Values		0.334	0.129	0.170	0.376	0.213	0.275	0.25

Figure 6 Effective thermal conductivity derived from the thermal response tests

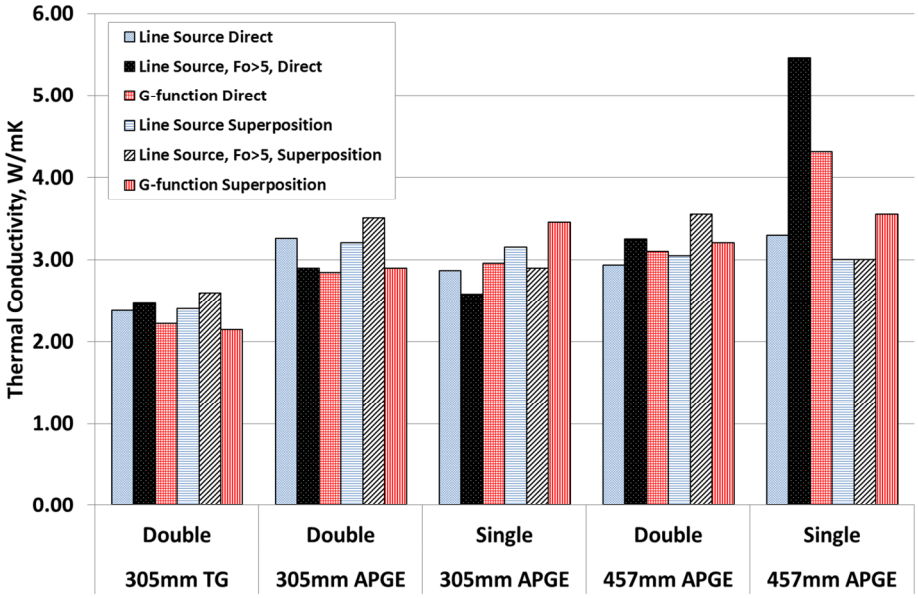

Figure 7 Pile thermal resistance derived from the thermal response tests

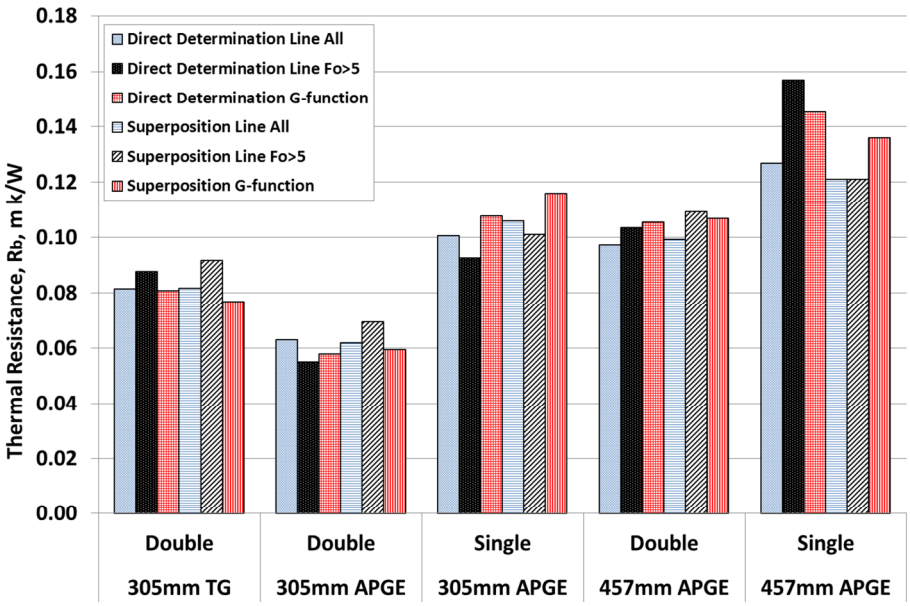

Figure 8 Root mean square error values for the model fits with the thermal response tests data

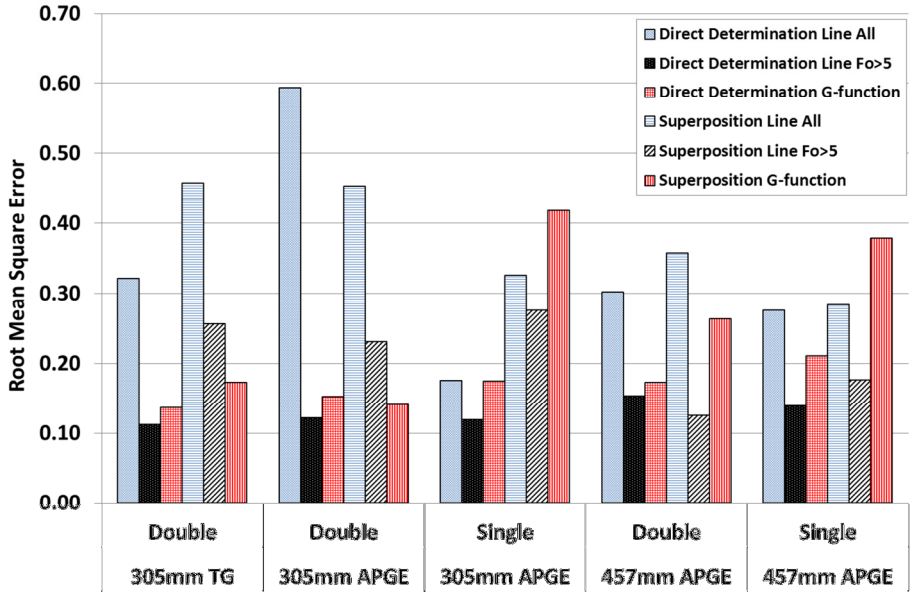

Figure 9 Model fits to test data – direct application of model: a) 305mm thermal grout pile – double, b) 305mm APGE pile – double, c) 305mm APGE pile – single, d) 457mm APGE pile – double, e) 457mm APGE pile – single

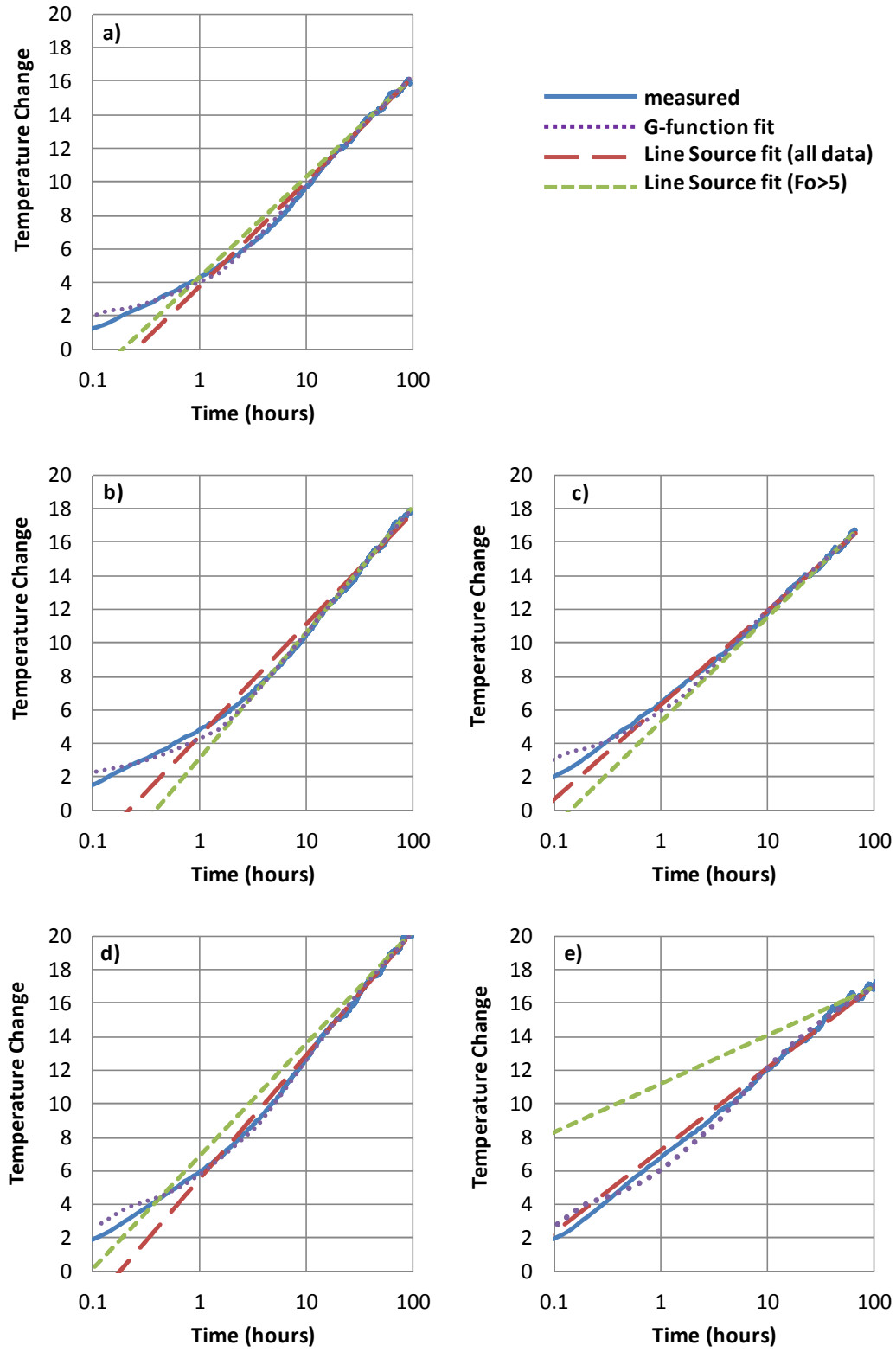

Figure 10 Model fits to test data – superposition approach: a) 305mm thermal grout pile – double, b) 305mm APGE pile – double, c) 305mm APGE pile – single, d) 457mm APGE pile – double, e) 457mm APGE pile – single

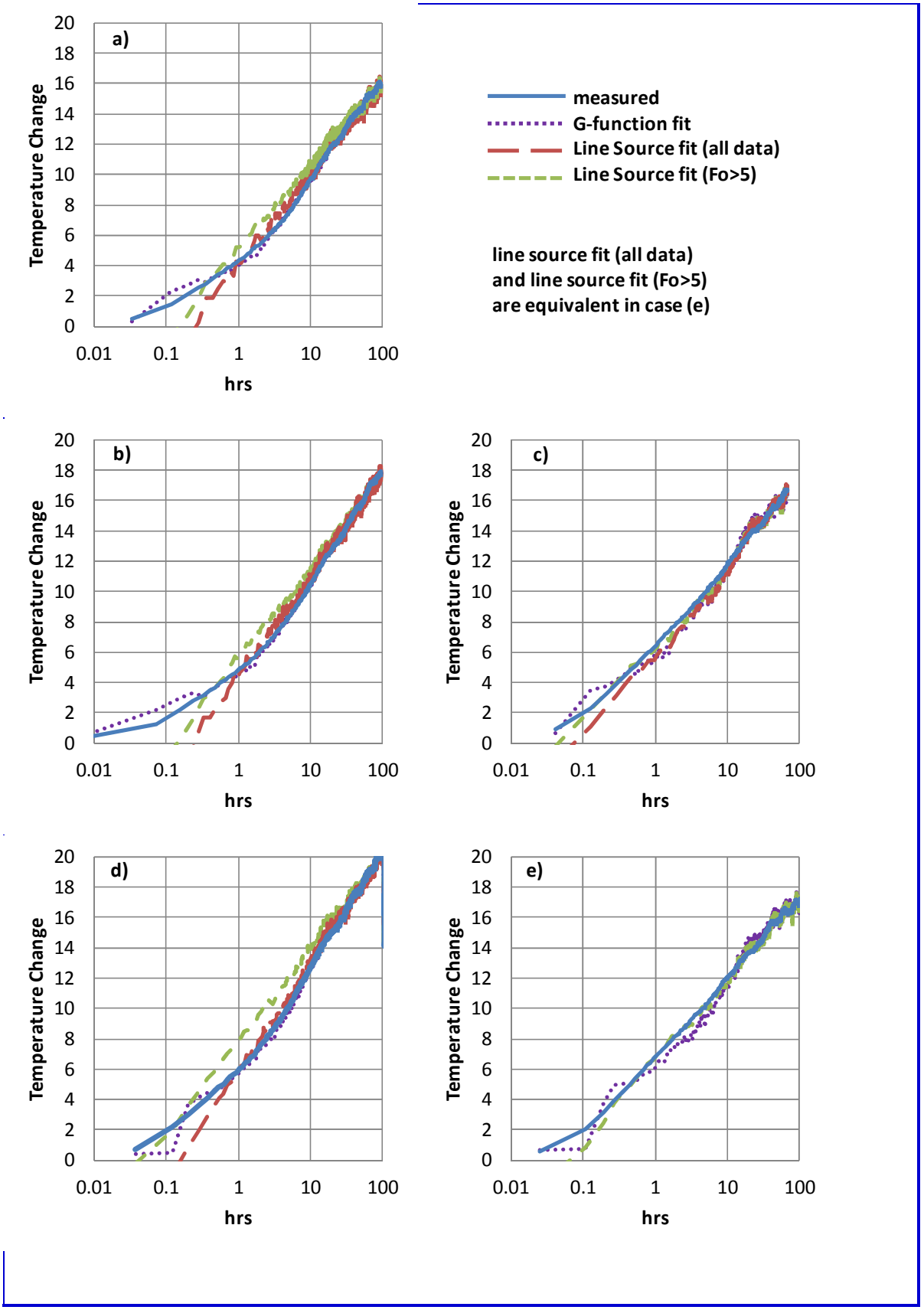

5.3 Grout Thermal Conductivity

It is possible to back calculate the thermal conductivity of the pile grouts from the values of thermal resistance determined from the thermal response tests. Using Equations 10 to 13, Figure 11 shows the relationship between grout thermal conductivity and pile thermal resistance for the Berkel and Company piles. For these calculations it has been assumed that the grout thermal conductivity is approximately half of the ground conductivity. While this may not be exactly true, for the arrangements of pipes in the piles being considered (which are closer to the pile centre than the edge), sensitivity analysis shows this factor to make only a very small (<2 %) difference to the outcome.

Using Figure 11, the thermal conductivity of the grout was determined for each of the four tests on the APGE piles (Table 8). These results are fairly consistent giving λ_c of 2.1 ± 0.1 W/mK. For the thermal grout, using the average thermal resistance value of 0.083 mK/W, the corresponding thermal conductivity is 1.6 W/mK. This value falls to 1.3 W/mK if a resistance of 0.1 mK/W is used in keeping with Figure 5.

Figure 11 Effect of grout conductivity on pile thermal resistance

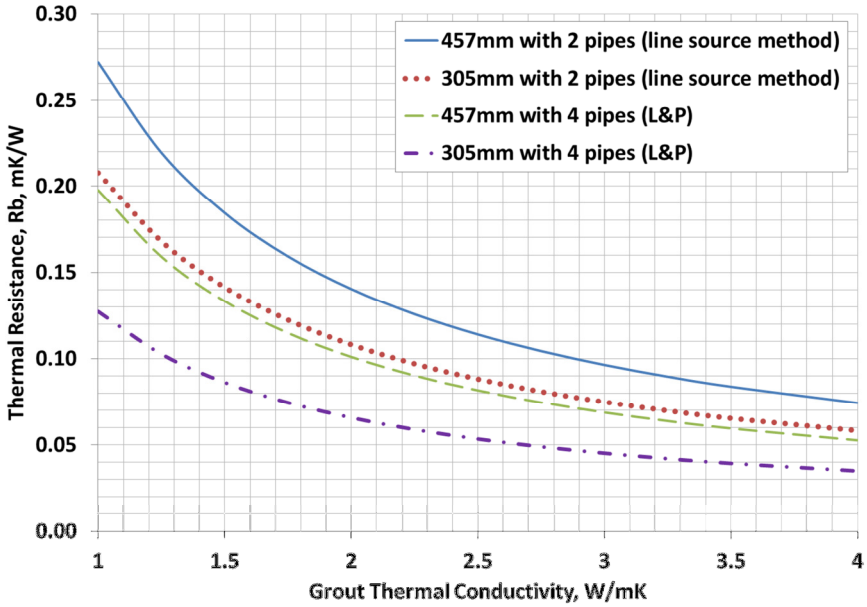

Table 8 Grout thermal conductivity determined from the thermal response tests

Pile	Loops	Average Pile Thermal Resistance (mK/W) from Table 6	Grout Thermal Conductivity (W/mK)
305mm TG	Double	0.08 0.10*	1.6 1.3
305mm APGE	Double	0.06	2.2
305mm APGE	Single	0.10	2.1
457mm APGE	Double	0.10	2.0
457mm APGE	Single	0.14	2.0

* based on Figure 5

6 Discussion

6.1 Factors Affecting Temperature Response

Three main factors are affecting the temperature response of the Berkel & Company piles. The first is pile diameter. The larger (18" or 457mm diameter) piles clearly take longer to reach a steady state and as a consequence a larger proportion of the initial data must be discarded when using the line source method of

interpretation. This means that the later period test data becomes more important. However, as the rate of change of temperature with time decreases into the test, power fluctuations have a proportionally larger effect later in the test. As a result, there is greater variation in the calculated thermal conductivity and thermal resistance values for the 457mm piles than for the 305mm diameter piles. This is also reflected in greater uncertainty attached to the results of the step-wise data interpretation for the 457mm piles, as reported in Loveridge et al. (2014a).

The second factor is the number and arrangement of pipes within the cross section. Where only a single loop has been tested, those 2 pipes are very close together. This means that their physical position and resulting behaviour is much closer to the theoretical line source, albeit not centred within the pile grout. In these cases the line source model gives a better fit to the measured data than the G-function model at short time periods. A similar result was seen by Loveridge et al. (2014b) when interpreting test data for a 300mm diameter test pile in London Clay with only one U-loop installed. In that case, the line source model also gave surprisingly good results. Although the two pipes were further apart for the London Clay pile, the ground and concrete conductivities were similar, which would have emphasised the line type behaviour.

However, when double loops were tested at the Berkel site, it can be seen in Figures 9 & 10 that the G-function models give a much better fit to the early time data, mirroring in particular the early curvature of the temperature response. This shows the influence of the pipe positions in controlling the rates of temperature change at small times.

The final factor that has been shown to have a large impact on the tests results presented is the thermal properties of the pile grout. While the cementitious APGE grouts behaved within the range of expectations, the thermal grout pile showed markedly different results. First, the ground effective thermal conductivity calculated from the TRT on this pile was much less that from the APGE piles, despite the ground conditions being the same. In addition, the value of pile thermal resistance calculated from the test was not consistent with the relative position of the temperature response curve in the other APGE tests (Figure 5). Back calculation of the grout thermal conductivity showed this to be approximately two thirds to three quarters that of the cementitious APGE grout. Combined with a low density (Table 2), this suggests that the thermal grout could have between one third and one half of the thermal diffusivity of the APGE grout. This would have a large impact on the transient behaviour of the pile, meaning that much longer testing periods would be required to obtain reliable thermal parameters from a TRT.

6.2 Comparison of Models

Previous experience has shown surprisingly good results from using the line source model with a 300mm diameter pile with a single U-loop (Loveridge et al., 2014b). A similar result is seen here with the single loop tests providing acceptable fits to the line source model. However, the G-functions clearly provide a better fit to the early time data where two U-loops are installed and potentially also for larger diameter piles. While the line source may still provide adequate results for the 457mm piles tests, there would need to be both a longer test and a stability of power supply, especially later in the test.

G-functions, however, also have other advantages. The line source model requires the early test data to be discarded, but as no test data set is ever perfect, the results then depend on precisely how much data is discarded. It is therefore beneficial to be able to use the entire test dataset, as is the case for the G-functions. This also makes it possible to use tests of shorter durations, which will have economic benefits. A further advantage of the G-function model is that it is applicable to piles of any aspect ratio. In the current cases the aspect ratios are quite high (AR=41 or 61), meaning that there is not too much divergence between the infinite line source and the pile G-functions during the latter part of the test (Figure 1). However, this divergence still results in the calculated thermal conductivities for the line source model (applied for Fo>5) being consistently higher than those for the G-function model. This difference is up to 10%, and would increase if the aspect ratio of the piles were larger. Similar discrepancies between the two models were observed by Loveridge et al. (2014b).

As a result of these factors the line source model can be used to reliably determine the effective thermal conductivity from a pile thermal response tests, but only when:

1. The pile diameter is small, certainly no more than 450mm, and possibly 300mm, depending on the other factors below.
2. Only two pipes are installed.
3. The concrete or grout thermal conductivity and diffusivity are large enough. Current experience suggests that this is likely to be the case for cementitious grouts or concrete, but not for low density grouts.
4. The test is carried out for long enough beyond Fo=5, with experience suggesting three to four days total duration being appropriate for 300mm diameter piles,
5. The pile aspect ratio is large. Values around 50 appear acceptable, but smaller values have yet to be tested.

Alternatively it is straightforward to implement directly the pile and concrete G-functions, which would be applicable for a wider range of pile geometries and shorter duration tests. Care must still be taken, however, with low thermal diffusivity grout materials.

The method of application of the models, direct or by superposition, also affects the results obtained. While direct application is simpler, the benefits of using superposition for the 457mm single loop test have been demonstrated. In this case, the power was highly variable and the test duration (for Fo>5) was short. However, it is interesting to note that for the other tests, the high degree of power variability made less of an impact on the results. This is despite the power variations (Table 2) being significantly greater than the limits recommended by ASHRAE for thermal response tests (ASHRAE, 2007). This suggests the potential for some relaxation of these requirements, but possibly only if the test duration is long enough.

6.3 Comparison with Laboratory Testing

The average of the thermal conductivity values derived from the thermal response tests was approximately 3.1 W/mK (selecting only reliable results). This compares favourably with the weighted average from the soil samples tests of 2.98 W/mK. For the grout, the laboratory results were 1.35 W/mK for both mixes. This was clearly an underestimate compared with the values derived from the TRTs. For the APGE grout this was calculated to be λ_c=2.1 W/mK and for the thermal grout λ_c=1.3 to 1.6 W/mK. It is not clear why there should be such a discrepancy between the two different types of grout tested.

In all case the laboratory tests give an underestimate of the thermal conductivity than the in situ results. This is consistent with previous studies by Low et al. (2014) and Olgun et al. (2014), although the magnitude of the underestimate is smaller in this case. The reasons for these discrepancies are unclear and research in this area is ongoing.

7 Conclusions

Thermal response testing of three auger pressure grouted (continuous flight auger) energy piles equipped with two U-loops each have shown the influence of three key parameters on the pile temperature response. These were pile diameter, the number and arrangements of the piping and the pile material thermal properties. The temperature changes across the pile tended to be larger when the pile was of larger diameter, the pile had fewer pipes installed and the pile was constructed with low thermal conductivity grout. These conditions would increase the pile thermal resistance and hence potentially reduce the efficiency of the associated ground energy system.

The pile thermal response tests were interpreted using two temperature response models: the infinite line source and pile and concrete G-functions. The line source model gave reasonable results provided that only two pipes (1 U-loop) were tested. However, the reliability of the results reduced as the pile size increased, the number of pipes increased and the thermal conductivity and thermal diffusivity of the pile grout decreased. The G-functions were found to give a better fit to the measured data when both U-loops were tested and for the larger diameter piles subject to power fluctuations. The use of G-functions in interpretation also offers the opportunity to carry out shorter tests, as there is no need to discard the early test data as when using the line source. This

effect becomes more significant for larger piles as the amount of data that has to be discarded is proportional to the square of the pile radius. Pile G-functions are also expected to perform better than the line source model as pile aspect ratio decreases and three dimensional effects become more important at shorter timescales.

Acknowledgements

This work has been carried out with support from the UK Engineering and Physical Science Research Council (research grant number EP/H049010/1). The second author was supported by the U.S. National Science Foundation under grants No. CMMI-0928807 and CMMI-1100752. The authors would also like to acknowledge Berkel & Company who funded the field testing and Jim Shaver who collected the test data.

References

ASHRAE (2007) *ASHRAE Handbook - Heating, Ventilating, and Air-Conditioning Applications*, American Society of Heating, Refrigeration and Air-Conditioning Engineers, Atlanta, 2007.

ASTM, (2008) Standard Test Method for Determination of Thermal Conductivity of Soil and Soft Rock by Thermal Needle Probe Procedure, ASTM D5334 – 08.

Bourne-Webb, P., Amatya, B., & Soga, K. (2013) A framework for understanding energy pile behaviour, *Proceedings of the Institution of Civil Engineering, Geotechnical Engineering*, 166(2), 170-177.

Bernier, M. (2001) Ground Coupled Heat Pump System Simulation, *ASHRAE Transactions*, 107 (1), 605-616.

Bennet, J., Claesson, J., Hellstrom, G. (1987) *Multipole method to compute the conductive heat flow to and between pipes in a composite cylinder*. Report. University of Lund, Department of Building and Mathematical Physics. Lund, Sweden.

Brandl, H. (2006) Energy foundations and other thermo active ground structures, *Geotechnique*, 56 (2), 81 – 122.

Brettmann, T., Amis, T. & Kapps, M. (2010). Thermal conductivity analysis of geothermal energy piles. Proceedings of the Geotechnical Challenges in Urban Regeneration Conference, London UK, 26 – 28 May 2010.

Brettmann, T.. & Amis, T. (2011) Thermal Conductivity Evaluation of a Pile Group using Geothermal Energy Piles. Proceedings of the Geo-Frontiers 2011 Conference, Dallas, Texas, March 13-16, 2011.

Carslaw, H. S. & Jaeger, J. C. (1959) *Conduction of Heat in Solids*. Second Edition, Oxford University Press.

Diao, N. R., Zeng, H. Y. & Fang, Z. H. (2004) Improvements in modelling of heat transfer in vertical ground heat exchangers, *HVAC&R Research*, 10 (4), 459-470.

Eskilson, P. (1987) *Thermal analysis of heat extraction boreholes*. Doctoral Thesis, Department of Mathematical Physics, University of Lund, Sweden.

Gao, J., Zhang, X., Liu, J., Li, K. & Yang, J. (2008) Thermal performance and ground temperature of vertical pile foundation heat exchangers: a case study, *Applied Thermal Engineering*, 28, 2295-2304.

Gnielinski, V. (1976) New equation for heat and mass transfer in turbulent pipe and channel flow, *International Chemical Engineering*, 16, 359 – 368.

GSHPA (2012) *Thermal pile design, installation and materials standard*, Ground Source Heat Pump Association, Milton Keynes, UK, October 2012.

Hellstrom, G. (1991) *Ground Heat Storage, Thermal Analysis of Duct Storage Systems, Theory*, Department of Mathematical Physics, University of Lund, Sweden.

Ingersoll, L. R., Zobel, O. J. & Ingersoll, A. C. (1954) *Heat Conduction with Engineering and Geological Applications*. 3rd Edition, New York, McGraw-Hill.

Javed, S. & Claesson, J. (2011) New analytical and numerical solutions for the short time analysis of vertical ground heat exchangers, *ASHRAE Transactions*, 117 (1), 13 – 21.

Koene, F. G. H., van Helden, W. G. J. & Romer, J. C. (2000) Energy piles as cost effective ground heat exchangers, In: Proc. TERRASTOCK 2000, Stuttgart, Germany, 28 August – 1 September. pp227-232.

Li, M. & Lai, A. C. K. (2012) New temperature response functions (G-functions) for pile and borehole ground heat exchangers based on composite-medium-line-source theory, *Energy*, 38, 255 – 263.

Loveridge, F. & Powrie, W. (2013) Temperature response functions (G-functions) for single pile heat exchangers, *Energy*, 57, 554 - 564.

Loveridge, F. & Powrie, W. (2014) On the thermal resistance of pile heat exchangers, *Geothermics*, 50, 122 – 135.

Loveridge, F., Brettmann, T., Olgun, C.G. & Powrie, W. (2014a) Assessing the applicability of thermal response testing to energy piles, DFI-EFFC International Conference on Piling and Deep Foundations, Stockholm, Sweden, 20-21 May 2014.

Loveridge, F., Powrie, W. & Nicholson, D. (2014b) Comparison of Two Different Models for Pile Thermal Response Test Interpretation, *Acta Geotechnica*, http://dx.doi.org/10.1007/s11440-014-0306-3.

Low, J., Loveridge, F., Powrie, W. And Nicholson, D. (2014). A comparison of laboratory and in situ methods to determine soil thermal conductivity for energy foundations applications, submitted to Acta Geotechnica.

Man, Y., Yang, H., Diao, N., Liu. & Fang, Z. (2010) A new model and analytical solutions for borehole and pile ground heat exchangers, *International Journal of Heat and Mass Transfer*, 53, 253-2601.

NHBC (2010) *Efficient design of piled foundations for low rise housing, design guide*, National House Building Council, Milton Keynes, UK.

Olgun, C.G., Ozudogru, T.Y., Brettmann, T. & Senol, A. (2014) 3D numerical evaluation of in-situ thermal conductivity tests performed on energy piles, submitted to Geothermics.

Pahud, D., & Hubbuch, M. (2007) Measured thermal performance of the energy pile system of the dock midfield of Zurich airport, In: Proceedings European Geothermal Congress 2007, Unterhaching, Germany, 30 May – 1 June.

Park, H., Lee, S-R., Yoon, S. & Choi, J-C. (2013) Evaluation of thermal response and performance of PHC energy pile: Field experiments and numerical simulation, *Applied Energy*, 103, 12 – 24.

Sauer, M. (2013) Evaluating improper response test data by using superposition of line source approximation, Proceedings of the European Geothermal Congress 2013, 3 – 7 June, Pisa, Italy.

Shonder, J.A., Beck, J.V., 2000. Field test of a new method for determining soil formation thermal conductivity and borehole resistance, *ASHRAE Transactions* 106 (2000) (1), pp. 843–850.

Zarrella, A., De Carli, M. & Galgaro, A. (2013) Thermal performance of two types of energy foundation pile: helical pipe and triple U-tube, *Applied Thermal Engineering*, 61, 301 – 310.